PSFC/JA-21-134

Width-Bending Characteristic of REBCO HTS Tape and Flat-Tape Rutherford-Type Cabling

Makoto Takayasu

July 17, 2021

Plasma Science and Fusion Center
Massachusetts Institute of Technology
Cambridge, MA 02139

This work was partially supported by the U. S. Department of Energy, Office of Fusion Energy Science under Grants: DE-FC02-93ER54186.

Submitted to Superconductor Science and Technology.

Abstract

The width-bending behaviors for a REBCO HTS tape have been investigated. It has been found experimentally that the width-bending strain of a YBCO tape does not degrade the critical current as much as is expected from the axial strain. The critical current is not directly affected by the width-bending strain but by the axial strain, which the width-bending strain generates by the Poisson effect. Since Poisson's ratio is about 0.3, the axial strain effective on the critical current is about 30% of the width-bending strain. Therefore, the width-bending strain of even 1.5% degrades the critical current by only 15% if the REBCO layer side is bent inward. However, the critical current degraded by more than 70% when the REBCO layer is outward. The width-bending effects on the critical current have been further examined, considering Poisson's ratio changes and the neutral plane shift of the REBCO tape substrate. Those changes would occur when the material yields due to severe width-bending. Based on the width-bending of REBCO tapes, flat-tape Rutherford-type cabling is discussed. A REBCO Rutherford-type cable can provide various advantages, especially for narrow-tape cabling. The flat-tape Rutherford-type cable has better characteristics against an electromagnetic transverse Lorentz force. Furthermore, the tape length of the cable can be approximately the same as the cable length allowing for excellent tape usage. REBCO Rutherford-type cabling will be a promising high-current, high-field cabling method using thin substrate REBCO tapes. It will be useful for AC ramp-field and pulse-field applications with low AC losses and low shield currents. It notes that the filaments in the cable are symmetrically distributed in parallel. Therefore, each filament's inductance is uniform, and a uniform current distribution among the filaments can be obtained.

Index Terms: High-Temperature Superconducting (HTS), bending strain, width bending, HTS cable, Rutherford cable, cable-in-conduit-conductor (CICC), REBCO superconducting magnet, superconducting power cable, fusion magnet, HEP magnet.

1. Introduction

High-temperature superconductors (HTS) such as BSCCO (Bismuth strontium calcium copper oxide) and REBCO (Rare Earth Barium Copper Oxide) tapes have excellent high-current performances at high fields. Therefore, they are desired for use in various electric device applications such as transformers, fault current limiters, magnets, energy storages, fusion, high energy physics devices, and power transmission cables. These practical applications demand high-current HTS cables.

The electrical current capacities of superconducting conductors can be increased with parallel operations of the wires. However, flux couplings created in the loop circuits among the superconducting wires generate AC losses (resistive and magnetic hysteresis losses) in the superconducting wires for AC or pulsed-field applications. A transposition technique of superconducting wires, such as twisting, has been used to reduce the magnetic flux coupling between superconducting wires. If the superconducting wires are round such as NbTi and Nb_3Sn wires, it is relatively simple to twist them along a cable axis. However, the twisting

transposition technology has not been readily applied to HTS superconducting thin flat tapes (typically 0.1 mm thick and 4 – 12 mm width). Therefore, various cabling methods for REBCO CC (coated conductor) have been developed, such as Roebel Assembled Coated Conductor (RACC), Conductor-On-Round Core (CORC®), Twisted Stacked-Tape Cable (TSTC), and a few other alternatives [1] – [12]. These HTS cable developments have been reviewed by Uglietti [13].

A cabling technique, so-called Rutherford cable, in which round wires are helically arranged and flattened into a rectangular cross-section, has been developed [14]. The technique has mainly been used for Low-Temperature Superconducting (LTS) round wires, such as NbTi and Nb_3Sn [15]. For round HTS BSCCO-2212 superconducting wires, high-current Rutherford-type cables have been manufactured [16]. For REBCO tapes, Roebel Assembled Coated Conductor (RACC) has been wound around a rectangular former to make a Rutherford-type cable at KIT [2], [17]. However, the Rutherford conductor required a bulky cabling former since the bending diameter of the RACC cable was limited to 10 mm – 15 mm. Consequently, the cable had an overall low current density. A Rutherford-type cable based on a TSTC [4] has also been fabricated for a high field and high current cable and successfully tested at PSI [7], [13].

The Rutherford-type cabling methods mentioned above were made in two steps; first fabricating sub-cables of REBCO tapes to fabricate a large-current multi-cable conductor. In this work, we intend to develop a novel flat-tape Rutherford-type cable by directly wounding flat REBCO tapes on a thin round-edge former.

This paper investigates a high-current REBCO CC cable using the Rutherford-type cabling (Flat Round-Edge Former Tape Cable, referred to as FReTC). Thin flat tapes are directly wound around a thin round-edge bar shape former with a relatively long twist-pitch (much longer than the cable width) to form a flat rectangular cable. This cabling method differs from the CORC® cabling referred to above, in which flat tapes are wound around a circular core with a relatively short twist-pitch resulting in an inefficient wire usage. Rutherford-type cabling has not yet been developed for a REBCO CC. A major obstacle for the flat cabling might be bending around sharp edges of the former, which might degrade the performance of superconducting tapes.

When a FReTC is fabricated by helically winding with a long twist-pitch around the former, REBCO tapes are forced to bend in the width direction ("width-bending") at the round edge of the former. To increase the current density of a cable, a thinner former is desired. Consequently, the width-bending strains increase and become critical for superconductor performances. However, we have found that width-bending strain affects the critical current of REBCO tapes differently from the axial-bending strain. This paper will first discuss the width-bending characteristics of a REBCO tape on the critical current based on our experimental results. Then the concept and design examples of FReTC will be discussed, including possible cable fabrication methods.

2. Width-bending characteristics of REBCO tape

2.1 Experimental

To apply width-bending to a REBCO tape in the width direction and to measure the critical current in liquid nitrogen, a special sample holder, shown in Fig. 1, was fabricated with

stainless steel by an Electrical Discharge Machining (EDM) wire cutting method. The sample holder was composed of the top and bottom pieces. An EDM cuts the boundary of a half-circle of a given diameter D_b. The cutting kerf width was about 0.37 mm. The tested REBCO tape was sandwiched between the top and bottom pieces and held with bolts, as seen in Fig. 2. Six different sample holders were fabricated, with the following bending diameters: D_b = 19.1 mm (3/4”), 12.7 mm (1/2”), 9.5 mm (3/8”), 6.4 mm (1/4”), 4.8 mm (3/16”), and 3.2 mm (1/8”). The smallest bending has an open slot at each side of the half-circle of the upper piece, as seen in the insert photo at the top right corner in Fig. 2, to prevent any tape damage. The length of the sample holder was 50.8 mm (2”). The REBCO tapes show permanent bending deformations for the small diameter bending, especially for bending D_b = 4.8 mm and 3.2 mm.

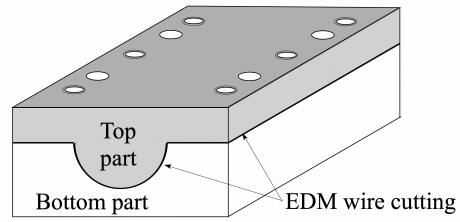

Fig. 1. Schematic view of a width-bending test sample holder to apply a bending to a REBCO tape in the width direction, made of stainless steel.

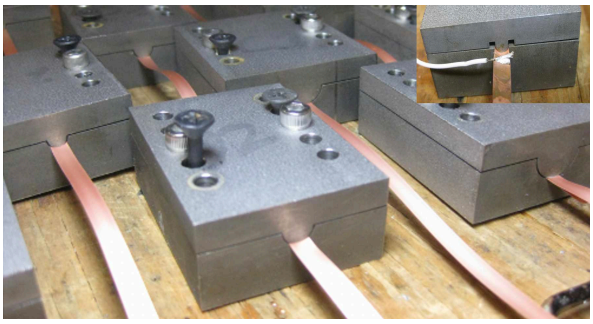

Fig. 2. 4 mm width REBCO tapes mounted on the width-bending strain sample holders. The insert shows the smallest bending-diameter sample holder.

Fig. 3 illustrates two different types of width-bending: (a) REBCO layer on the outer surface of the width bent tape, (b) REBCO layer on the inner surface. An actual REBCO tape has a copper layer on each side additionally, but in the figure, they are not shown. When a width-bending is applied to a tape, the outer and inner REBCO layers on the substrate are at the tension side and the compression side, respectively.

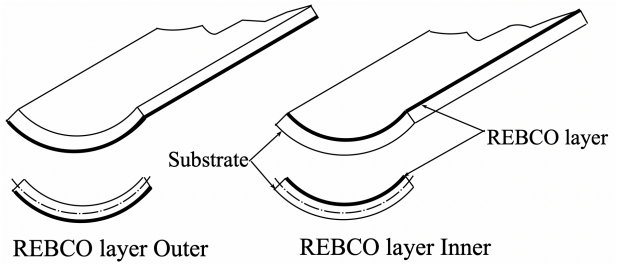

Fig. 3. Illustrations of REBCO tapes applied width-bending. (a) REBCO layer outward, (b) REBCO layer inward.

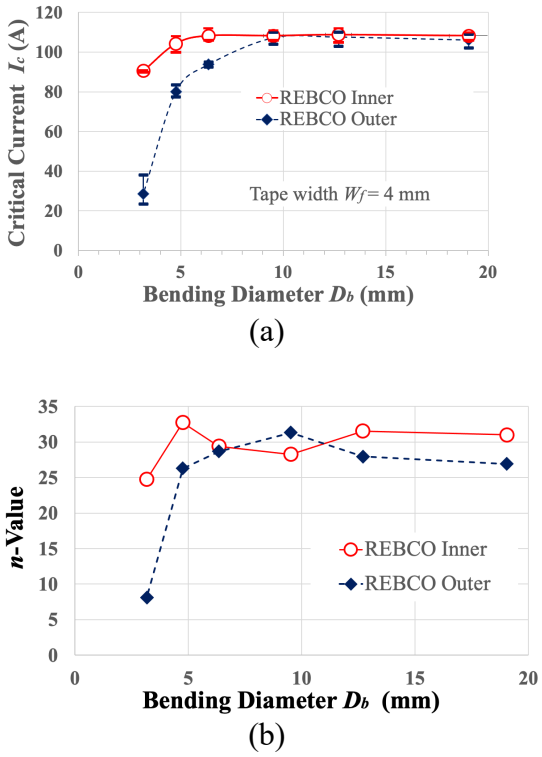

Fig. 4. Width-bending experimental results for SuperPower 4 mm width YBCO SCS4050-AP measure at self-field in liquid nitrogen. (a) The critical currents as a function of the bending diameter (bar marks represent the maximum and minimum values among four measured data), and (b) the n-values.

The critical current test was performed using the YBCO tapes of SuperPower SCS4050-AP, purchased in 2012. The tape width and the substrate (Hastelloy C-276) thickness were 4 mm and 0.05 mm, respectively. A copper layer of about 0.02 mm thickness was electroplated around the tape, according to the manufacturer.

Test results of the critical current I_c are shown in Fig. 4(a). Each data point was an average of four samples tested in the same condition. Bar marks show the maximum and minimum values among the four. The critical currents were measured at self-field in liquid nitrogen. The

critical current was evaluated at the criterion of 100 μV/m with the voltage tap separation of 54 mm. The n-value was obtained between the 100 μV/m and 1000 μV/m criteria.

The open circles (red line) in Fig. 4(a) were obtained for the REBCO layer mounted in-side (REBCO Inner, Fig. 3(b)). In comparison, the solid diamond marks (blue line) were for the out-side (REBCO Outer, Fig. 3(a)). A significant difference in the critical current due to the REBCO layer locations of the width-bending can be seen when the bending diameter is smaller than 9 mm. The critical current of the REBCO Outer sharply degrades for a width-bending less than 5 mm bending diameters, while the critical current of the REBCO Inner degraded for a 3.2 mm bending diameter only by about 15%. The n-values for the measured critical currents in Fig 4(b) were about 29, except n= 9.4 at D_b =3.2 mm for the REBCO Outer, which indicated a severe critical current degradation. The experimental results of the REBCO tapes tested indicate that a FReTC cabling for a REBCO flat tape should be fabricated in the REBCO Inner configuration.

2.2. Theoretical analysis of width-bending

Since REBCO layer thickness is thin enough compared to the substrate, the bending strain of the REBCO can be approximated to the strain of the substrate surface. Therefore, the bending strain ε_b of a REBCO layer on a substrate is given in the pure bending model by [18],

$$\varepsilon_b = \frac{s_t}{D_b} \tag{1}$$

Where s_t is the thickness of the substrate, and D_b is the bending diameter. In this equation, the neutral plane of the bending is at the middle plane of the substrate.

Fig. 5 shows the width-bending strains calculated for the REBCO tape for a substrate thickness of 0.05 mm as a function of the bending diameters used for the above tests. The bending strains applied to the REBCO layers reached a strain as high as 1.5%. The width-bending strains are beyond the elastic region and in the range for yielding. When the width-bending is applied to the REBCO tapes, a strain is induced in the axial direction due to the Poisson effect. The axial strain ε_a can be evaluated with a given Poisson's ratio ν_p of the substrate material by

$$\varepsilon_a = -\nu_p \, \varepsilon_b \tag{2}$$

Fig. 5 also plots two lines marked with solid triangular and square, obtained with Poisson's ratios of 0.3 and 0.5, respectively. Poisson's ratios of stainless steel and copper are about 0.3 [19]. The theoretical maximum value of Poison's ratio is known to be 0.5 [20]. These lines show the absolute strain values (both tensile and compressive strains). They are the strains on the substrate surface, which should be the strain of the REBCO layer due to the width-bending.

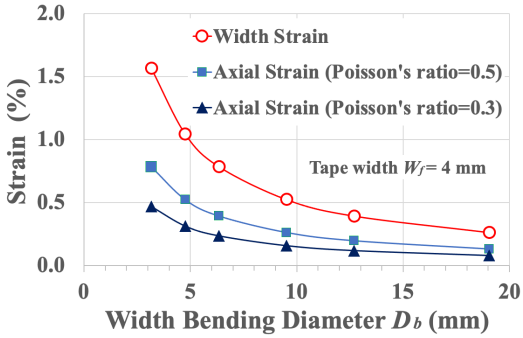

Fig. 5. Calculated stains of the REBCO layer due to the width-bending for a substrate thickness of 0.05 mm. The width-bending strains (Red line) were obtained under a pure bending model. The corresponding axial strains in the REBCO tape are plotted with the black line (triangular marks) and the blue line (square marks) calculated with 0.3 and 0.5 of Poisson's ratios, respectively. These strains are absolute values showing for both tensional and compressive strains.

2.3 Critical current simulation model

The critical currents experimentally obtained in Fig. 4 could not be fitted by the axial strain evaluated by (2) with Poisson's ratio of 0.3. The critical current degradation for the REBCO Outer sharply increased with the bending strains, while that for the REBCO Inner showed a slightly larger degradation than the expectations from the axial strains (2) with the Poisson's ratio of 0.3.

Similar experimental phenomena were observed in the past for pure-bending critical-current tests of Nb_3Sn multifilament superconducting wires [21]. They were evaluated considering four effects: neutral axis shift, current transfer length, filament breakage, and uniaxial strain release. From the analogy, we will examine the REBCO bending characteristics considering Poisson's ratio variation and neutral plane shift. The Poisson's ratio variation is a unique model for a REBCO tape experiencing a severe width-bending causing a strain that exceeds the elastic strain region.

Poisson's ratio variation

In general, for isotropic materials, Poisson's ratio ν_p is given as [20],

$$\nu_p = \frac{1}{2} - \frac{E}{6K} \tag{3}$$

where K is the bulk modulus, and E is Young's modulus.

Poisson's ratio is constant in the elastic region of linear strain-stress behavior, but it varies outside the linear range under a severe width-bending. After reaching yielding, Young's modulus becomes small in the plastic region. Accordingly, from (3), the Poisson's ratio increases toward the maximum value of 0.5 for Young's modulus $E = 0$. With decreasing the width-bending diameter, the Poisson's ratio could increase from 0.3 to ~ 0.5 due to plastic deformation.

Neutral plane shift

The neutral plane of a width-bending is at the center in an elastic material. However, , it is possible that the neutral axis shifts towards the compressive side due to material yielding, as done for an Nb_3Sn round superconducting wire [21 – 24]. In the same way, the neutral plane in a REBCO tape can shift due to severe bending since the substrate material yielding is not linear over the tension and compression regions through the tape thickness.

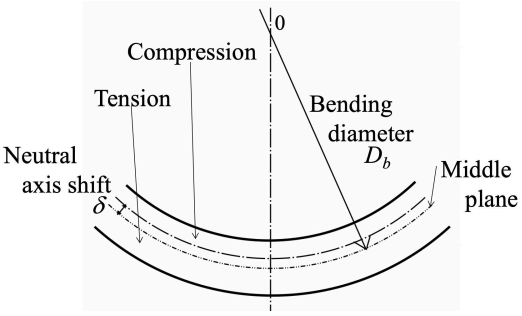

Fig. 6. Illustration of a neutral plane shift in a cross-section of REBCO tape substrate. Copper layers on both sides of the substrate are not shown.

If the neutral plane shifts towards the compressive side by δ (as shown in Fig. 6), the bending strain (1) can be modified as,

$$\varepsilon_b = \frac{s_t+2\delta}{D_b-2\delta} \tag{4}$$

Poisson's ratio and the neutral plane shift have not been obtained experimentally. Therefore, we will estimate them by curve-fitting the critical current.

Critical-current curve-fitting

Experimental critical current data for the strains between -1.9% and +0.6% have been reported for the SuperPower YBCO tape similar to the one used for the present test [25]. The critical currents results showed the maximum value at the tension strain ε_a = 0.15%. The reported data points normalized by the critical current I_{co} at ε_a = 0.15% were fitted by the following polynomial equation (5) using Microsoft Excel® curve-fitting function.

$$I_c/I_{co}(\varepsilon_a = 0.15\%) \approx -0.080706\text{x}10^{12}\ \varepsilon_a^6 - 0.312419\text{x}10^{10}\ \varepsilon_a^5 - 0.213264\text{x}10^{8}\ \varepsilon_a^4 + 0.123439\text{x}10^{6}\ \varepsilon_a^3 - 0.305822\text{x}10^{4}\ \varepsilon_a^2 + 0.078479\text{x}10^{2}\ \varepsilon_a + 0.990632 \tag{5}$$

Equation (5) was used to evaluate the critical current behavior of the tested YBCO tapes experiencing width-bending.

2.4 Critical current simulation

The measured critical currents were fitted by (5), where the strain ε_a (%) was obtained by adjusting the neutral plane shift δ (mm) in (4) and Poisson's ratio in (2).

The resulting fitting curves are shown in Fig. 7 with a dotted line for REBCO Inner and a dashed line for the REBCO Outer. The experimental results of the critical currents in Fig. 4 were normalized by an initial critical current I_{co} of 107 A.

During the curve fitting, it was found that the Poisson's ratios were very similar for both cases of the REBCO Inner and Outer, as shown in Fig.8(a). The resulting Poisson's ratios are plotted as a function of the bending diameter. The Poisson's ratios monotonically increased to 0.48 with decreasing the bending diameter below a 10 mm diameter, while it was a constant of 0.3 above ~10 mm. Following these results, the same Poisson's ratio values were used for both cases.

The neutral plane shift started to increase at ~10 mm bending diameter and reached maximum values of 0.018 mm for the REBCO Outer and 0.002 mm for the REBCO Inner at the 3.2 mm bending diameter (Fig. 8(b)). Thus, the REBCO Outer case showed a significant neutral plane shift.

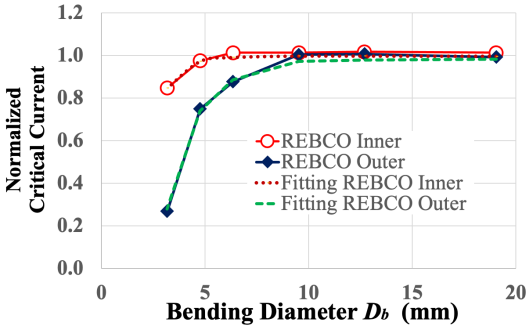

Fig. 7. Curve fitting of the critical current measured for the width-bending tests of REBCO layer inward and outward. Fitted curves are shown with a dotted line for REBCO Inner and a dashed line for REBCO outer.

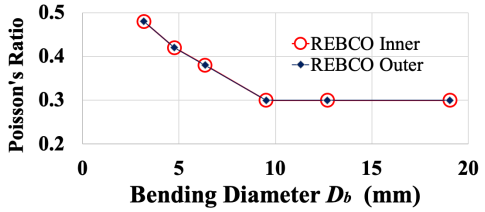

(a)

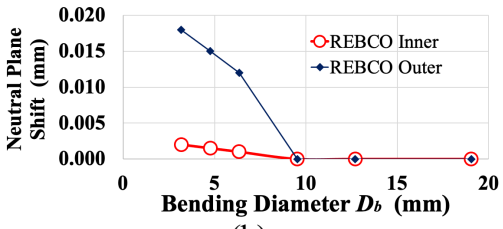

(b)

Fig. 8. Fitting parameters used for the curve fitting of the critical currents shown in Fig. 7 are plotted: (a) Poisson's ratio and (b) the neutral plane shift.

2.5 Width-bending strain effects on the critical current

Fig. 9 replotted the test results of the critical currents (Fig. 4) and the analytical fitted results (Figs. 7 and 8) as a function of the width-bending strains (absolute value) obtained by the pure bending formula (1). The width-bending strain applied was more than 1.5%, but the critical current degradation was only 15% for the REBCO Inner bending. However, the REBCO Outer bending resulted in more than 70% critical current degradation. The critical current degradation has been examined considering the yielding of the substrate, the Poisson effect, and the neutral plane shift.

The width strains and axial strains estimated for the critical current curve fitting were plotted in Fig. 10. The estimated width strain was obtained with the neutral plane shift δ by (4). The estimated axial strain was calculated from (2) using the estimated width strain and the estimated Poisson's ratio shown in Fig. 9. The estimated width strain for the REBCO Outer bending exceeded 2.6%, corresponding to the significant neutral plane shift. The axial strain was -1.3%. It resulted in a significant critical current degradation at D_b =3.2 mm. On the other hand, the estimated width and axial strains for the REBCO Inner bending at D_b =3.2 mm were -1.4% and 0.67%, respectively.

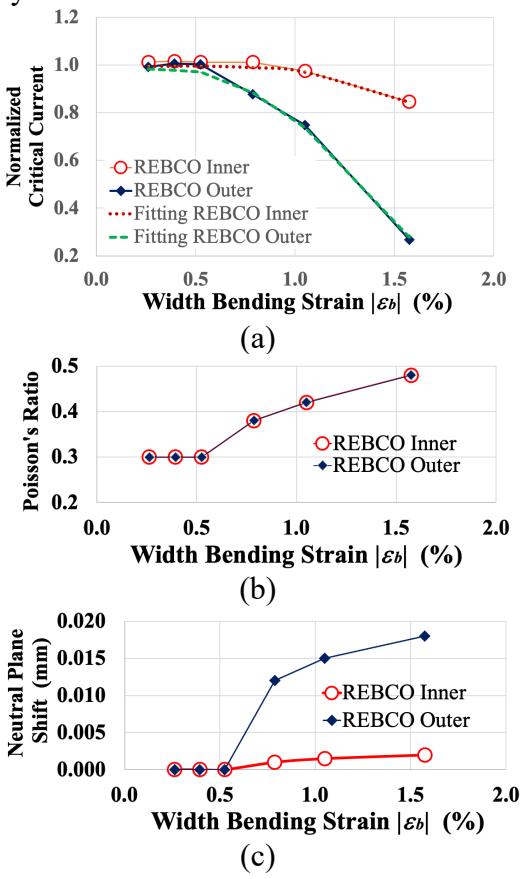

Fig. 9. (a) Normalized critical currents obtained experimentally and the fitted curves (shown by dotted lines) calculated using the fitting parameters of (b) Poisson's ratio and (c) the neutral plane shift. All quantities are plotted as a function of the width-bending strain.

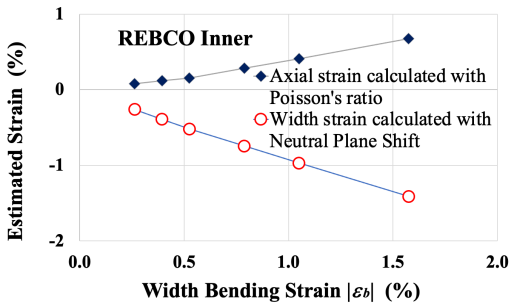

(a)

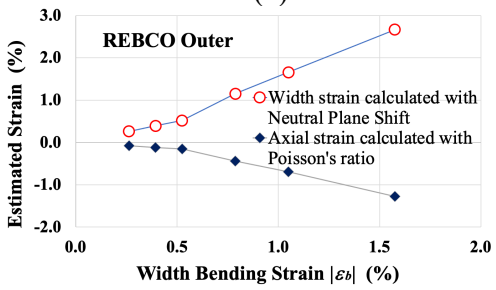

(b)

Fig. 10. Estimated width-strain and axial-strain used for the curve fitting of the critical currents of (a) REBCO Inner and (b) REBCO Outer bending.

When the material yields through an elastic-to-plastic transition due to severe width-bending, the Poisson effect will not be a linear phenomenon with a constant value of Poisson's ratio. Thus, the bending characteristic differs from that of the pure bending theory. For the wide range of the width-bending applied to the YBCO tapes, the Poisson's ratio change and the neutral plane shift have been evaluated by the critical current fitting, as shown in Figs. 7, 8, 9, and 10. The nonlinear transition of the evaluated Poisson's ratio and neutral plane shift started above the width-bending strain of 0.5% for both REBCO Inner and Outer.

The substrate of the SuperPower YBCO tape was Hastelloy C-276. Its yield strength was reported to be 700 MPa at 0.35% at 76 K [26]. The yield point of a YBCO tape (SuperPower) is about the stress of 750 MPa at 0.8% at 4 K [27]. These yield points of Hastelloy and YBCO tape agreed well with the strains showing nonlinearities of Poisson's ratio in Fig. 9(b) and the neutral plane shift in Fig. 9(c). The trends of Poisson's ratios of REBCO Inner and Outer fittings were similar since the Poisson's ratio might be a bulk property.

The neutral plane shifts showed different trends, as seen in Fig. 9(c). The neutral plane shift was evaluated to calculate the surface bending strain of the substrate by (4). The neutral plane shift value may not be an actual value, but the bending strain at the substrate surface can be obtained from (4) using the neutral plane shift value.

The nonlinearity of the compress region differs from that of the tension region. The neutral plane shifts toward the center of the bending curvature, since the neutral center is established by a force balance between the compression and tension regions, and the elastic-to-plastic transition occurs in the tension region before the compression region [28]. Therefore, the neutral plane shift of REBCO Inner is not the same as that of REBCO Outer, as seen in Fig. 9(c). It is important to note that the internal stress-strain characteristics is not linear. Therefore,

the equation (4) cannot be used with a constant value of δ. Different neutral plane shift values should be used to obtain the bending strain at the tension and compression surface using (4). The results presented clearly show that the REBCO Outer bending degrades the critical current significantly due to severe width-bending in the tension stress region. In contrast, the strain development due to the width-bending in the compression region (REBCO Inner) is less than in the tension region (REBCO Outer). Therefore, it results in less critical-current degradation for the REBCO Inner bending.

2.6 Summary of width-bending

The width-bending strain of a YBCO tape did not show much critical current degradation as expected from the axial strain effect, although the tested width-bending strains were as high as ±1.5%. Thus, the critical current seems not to be directly affected by the width-bending strain strength. The effective strain on the critical current is more likely influenced by the axial strain, which the width-bending strain generates through the Poisson effect. The induced axial strain is about 30% of the width-bending strain since Poisson's ratio is about 0.3.

When the REBCO layer side is bent inward, the width-bending strain of 1.5% degraded the critical current by only 15%. On the other hand, the critical current degraded by more than 70% when the REBCO layer is outward. The width-bending effects on the critical current have been examined considering Poisson's ratio changes and the neutral plane shift of the tape substrate, corresponding to substrate material yielding due to severe width-bending. The critical current degradations have been quantitatively formulated using those factors. One can consider other origins. For instance, Okada et al. recently reported that the twin-structure in-plane ratio of the a-axis and b-axis domains aligned in the longitudinal direction of REBCO CC was varied over time even at room temperature by applying a compressive bending strain [29]. Consequently, bending strains affect the critical current due to the domain change. It is an interesting phenomenon for future developments of the cabling. Since REBCO CC is a ceramic layer deposited on multiple buffer layers established on a metallic substrate, mechanical behaviors of the REBCO layer due to excess bending will be complicated due to various factors. We may need to consider mechanical damages such as micro-cracking due to severe bending, like filament breakage due to bending for Nb_3Sn wires [21].

Our experimental work was performed only with 50 μm substrate YBCO tapes of SuperPower at self-field in liquid nitrogen. To reduce width-bending strains and fabricate a FReTC conductor without significant degradation, thinner substrate REBCO tapes and STAR wires recently developed [30] will be used.

3. Flat Round-Edge Former Tape Cabling (FReTC)

3.1. Preliminary flat round-edge former tape cabling test

To fabricate a preliminary flat round-edge former tape cabling (FReTC), four 4-mm width YBCO tapes (SuperPower YBCO SCS4050-AP) were mounted with a twist-pitch of 200 mm on a 12.7 mm (½") width, 4.8 mm (3/16") thick aluminum round-edge bar (used as the flat-cabling former), as shown in Fig. 11. The REBCO tape was tightly held on the aluminum bar surface with a flat wraparound tape (Nomex® lacing tape) so that the REBCO tape was bent in the width direction (width-bending) at the round-edge. The length of each of the four YBCO tapes was 1100 mm, including the terminations. The 700 mm long sections of the tapes were mounted on the aluminum bar. The tapes were terminated separately to measure their critical

currents. The critical currents were measured with voltage tap-separations of 500 mm and 250 mm for each tape. The voltage taps were soldered on the tape surface. The results of each tape were plotted with four large open circles in Fig. 12, where two critical current values for each tape obtained for 500 mm and 250 mm voltage taps were averaged. Therefore, four open circles are seen at the bending diameter D_b = 4.8 mm. The average critical current and the standard deviation of 8 measured I_c values were 107.8 A and 1.30 A, respectively. In Fig. 12, the tape data of Fig. 4(a) were re-plotted for comparison. They were very consistent without degradations due to the cabling and agreed well with the tape data.

Fig. 11. Four 4 mm width REBCO tapes wound on a 12.7 mm width, 4.8 mm thick aluminum round-edge bar of the flat-cabling former. The insert shows a cross-section of the round-edge bar.

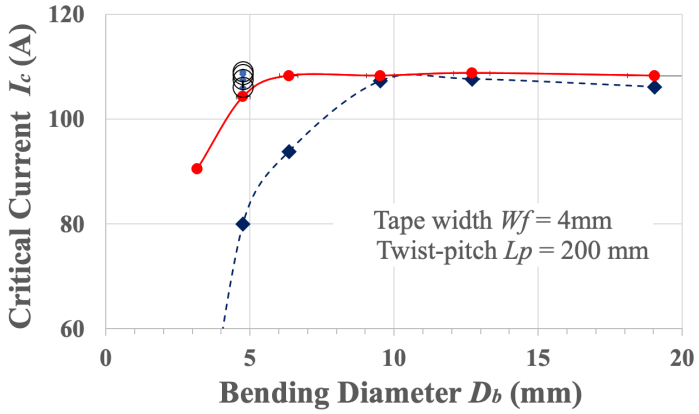

Fig. 12. Four large circles showing experimentally obtained critical currents for the four tapes mounted on the round-edge bar. The tape data in Fig. 4(a) are also shown for comparison.

3.2 Cable topology of FReTC

A FReTC cabling applies a sharp bending on the superconducting tape in the tape width direction (width-bending) during cabling. However, REBCO tapes do not degrade much if the REBCO layer is mounted inward, as discussed above. Fig. 4 shows that a round-edge of 3.2

mm diameter degrades the critical current about by 15% for REBCO Inner cabling. Therefore, it will be possible to fabricate a FReTC conductor using flat REBCO tapes.

Fig. 13 shows a flat tape (filament) of the width w_f wound helically on a round-edge bar former (the width of W_c). The helically twisted tape has the twist-pitch L_p and the twist-pitch angle α. The side corners of the former are rounded to avoid sharp bending. The perpendicular tape width to the former axis is $w_f/cos\alpha$, and the tape length covering the round-edge corner is $\pi R_e/sin\alpha$.

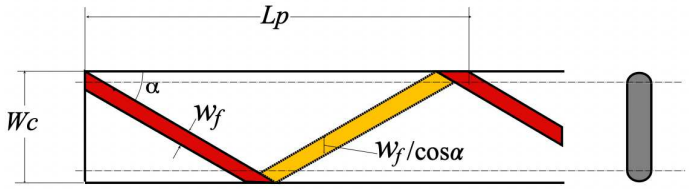

Fig. 13. A flat tape of the width w_f wound helically on a round-edge bar former of the width W_c with the twist angle α.

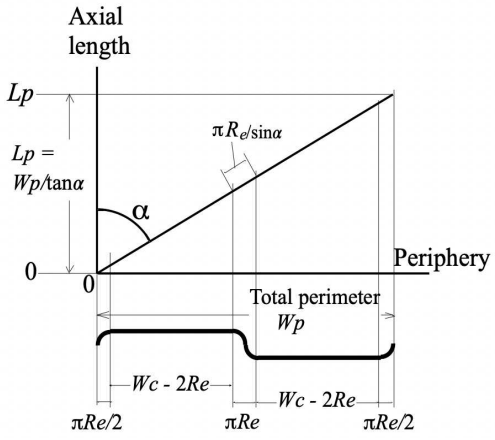

Fig. 14. A graphic illustration of the tape length as a function of the periphery of the former. The corner radius of the former is R_e. α is the twist angle.

Fig. 14 illustrated a linear relation of the tape length as a function of the periphery of the former, taking into account the rounding corners of the former. The corner radius of the former is R_e ($R_e = D_b/2$).

The perimeter of the rectangular shape former, W_p, and the twist angle α are given,

$$W_p = 2(W_c - 2R_e + \pi R_e) \tag{6}$$

$$\approx 2W_c \qquad \text{if } R_e << W_c \tag{7}$$

$$\tan\alpha = W_p / L_p \tag{8}$$

The maximum filament number n_{max} for a tight winding (100% surface coverage) is,

$$n_{max} = Lp \sin\alpha / w_f \tag{9}$$
$$= W_p \cos\alpha / w_f \tag{10}$$
$$\approx 2W_c \cos\alpha / w_f \qquad \text{if } R_e << W_c \tag{11}$$

Tape length and cable length

The tape length wound helically on a former as seen in Fig. 13 is given per a twist pitch by:

$$\sqrt{{L_p}^2 + 4{W_c}^2} \tag{12}$$

The ratio of the tape length to the cable length is written as;

$$\sqrt{{L_p}^2 + 4{W_c}^2}/L_p = \sqrt{1 + 4(W_c / L_p)^2} \tag{13}$$
$$\approx 1 + 2\,(W_c / L_p)^2 \qquad \text{if } W_c << L_p \tag{14}$$

The tape length ratios to the cable length for the twist-pitches up to 1000 mm with various former widths are plotted in Fig. 15. For the twist-pitch of 200 mm, the ratios are 1.005 and 1.02 for the former widths of 10 mm and 20 mm, respectively. Note that the tape lengths for these cables are approximately the same as the cable length if the twist-pitch is more than 200 mm. Thus, the tape length of a FReTC is practically the same as the cable length like a Twisted Stacked-Tape Cable (TSTC), and unlike a CORC® cable, in which the tape length required is much longer than that of the cable length due to the tight twist pitches [4].

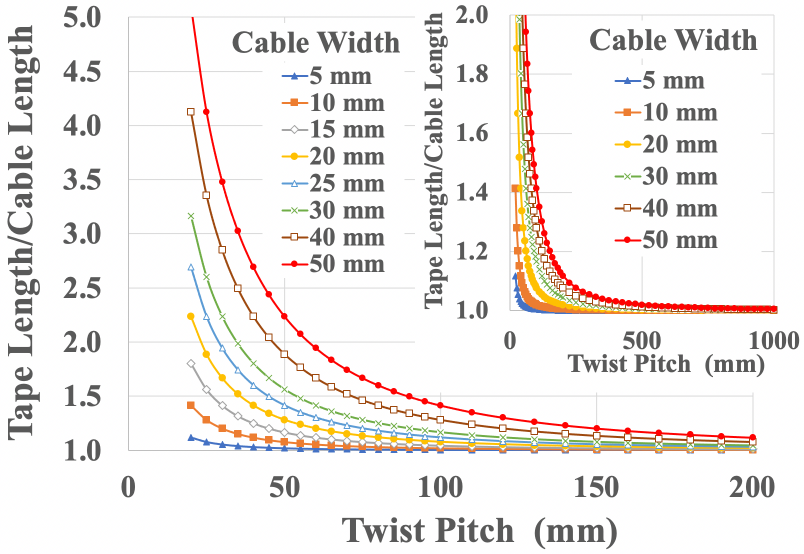

Fig. 15. Tape usage of a flat round-edge former tape cable (FReTC) plotted the ratio of the tape length to the cable length for the twist-pitches up to 1000 mm with the various widths of the former.

3.3 FReTC design examples

Design parameters of a FReTC are defined as follows. Symbols described above are also summarized below;

N = the number of the total strand (bundled filament) in a cable
n_s = the number of the filament in a strand
n_t = the number of the total filament in a cable, $n_t = N^* n_s$
L_p = the twist pitch
W_c = the cable former width
R_e = the radius of the former corner
W_p = the perimeter of the rectangular shape former
w_f = the filament width

Commonly, 2 mm to 6 mm width wires of REBCO flat tapes have been fabricated from a wider tape such as a 10 mm to 20 mm width tape by slitting [31]. A tape can be wound on a rounded edge former. Also, a bundled tapes (strand) of narrow slitted tapes (filament) or a wide tape with narrow superconducting layers striated on one substrate can be wound. In this way, the narrow tapes will be easily handled for cabling. Three examples of FReTC for REBCO tapes are illustrated in Fig. 16;

(a) 10 filaments in a bundled strand
(b) Two strands of 5-filaments
(c) Four strands of 5-filaments

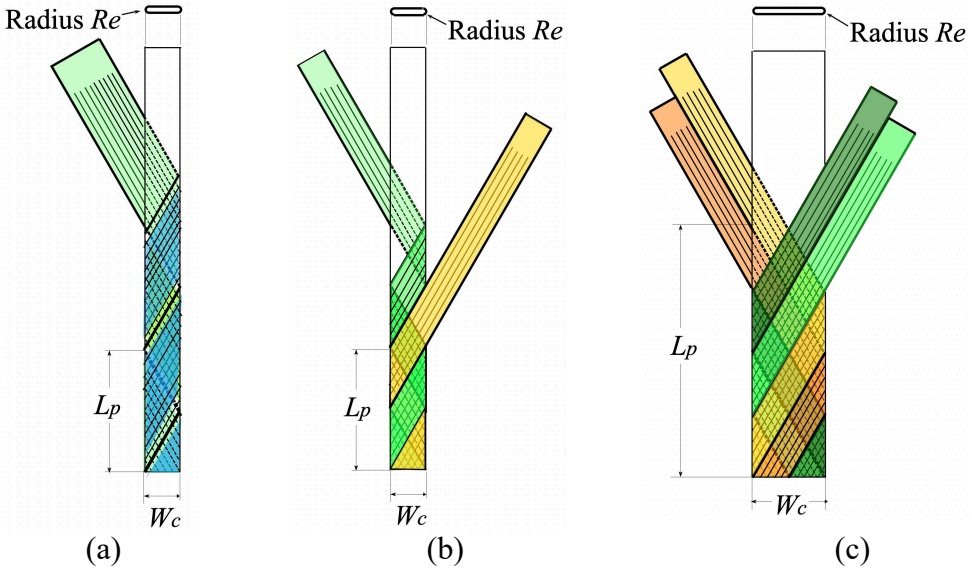

Fig. 16. FReTC conductors: (a) 10 filaments in one bundled strand, (b) two strands of 5-filaments in each strand, and (c) four strands of 5-filaments in each strand.

Table I shows the typical design parameters of the three cables in Fig. 16. The cable critical currents are evaluated using the critical current 50 A for 1 mm width filament at 77 K in self-field. The critical current value is approximately the same as that at the temperature of 4.2 K in the field 18 T.

Table I. Cable design parameters of the cables shown in Fig. 16.

Cables	a	b	c
The number of strands in a single layer N	1	2	4
The number of filaments in a strand n_s	10	5	5
The number of the total filaments in a single layer cable n_t	10	10	20
Twist pitch (mm)	200	200	200
Surface coverage of the filaments (%)	100	100	100
Layer critical current* *Ict* (A)	500	500	1000
Multiple-layer cable			
The number of layers in a cable N_m	8	48	72
The number of the total filaments in a cable n_f	50	300	1,000
Filament width (mm)	1	1	1
Former thickness (mm)	2.5	2.5	2.5
Former width (mm)	3.86	3.86	8.91
Critical current* *Ic-cable* (A)	4,000	24,000	72,000
Engineering Current density** *Je* (A/mm^2)	315.8	590.2	698.9

* Note: Filament 1 mm width, I_c = 50 A at 77 K at cable self-field or at 18 T at 4.2 K.
** Note: Former thickness 2.5 mm and tape thickness 0.035 mm (substrate thickness 0.025 mm). The current density for the former and the REBCO tapes without insulation and jacket.

The former thickness of 2.5 mm was used in Table I, which is much thinner than that used for the experiment in Figs. 11 and 12. From Fig. 4, we have found that the bending diameter (the former thickness) of 4.76 mm did not significantly degrade the critical current for the REBCO tape substrate thickness of 0.05 mm. Therefore, a REBCO tape of the substrate 0.025 mm thick (under development at SuperPower) for the former thickness of 2.5 mm is expected to behave even better and have less degradation than the experimental results shown in Fig. 4, since the bending strain is given by the ratio of the substrate thickness and the bending diameter (the former thickness) from (1).

Fig. 16 shows single-layer cablings of the FReTC conductors. Multiple layer windings can be fabricated for a high-current cable in the same way. The multiple-layer cable designs (the number of layers in a cable N_m) are also shown in Table I. For example, 8 layers of Fig. 16(a), 48 layers of Fig. 16(b), and 72 layers of Fig. 16(c) can provide 4 kA, 24 kA, and 72 kA, respectively. The engineering current densities J_e of the cables (a), (b), and (c) for the former thickness of 2.5 mm and the tape thickness of 0.035 mm (substrate thickness 0.025 mm) without insulation and jacket are 315.8 A/mm^2, 590.2 A/mm^2, and 698.9 A/mm^2, respectively. Therefore, a REBCO FReTC conductor can achieve a high critical current density.

Table II shows other flat-tape cable examples designed for 4 mm width tapes which is the same tape used for the tape tests shown in Figs. 4 and 11. The tape thickness is 0.095 mm, and the substrate thickness is 0.05 mm. The former thickness is 4.76 mm. The former widths of the cables were obtained to make the surface coverage of the tapes 100%. Table II (a) shows four 4 mm width tapes used for the first layer, which were wound on the former of 5.31 mm width x 4.76 mm thickness, and the five layers provides 4 kA cable at 18 T at 4.2 K. Table II (b) and (c) show 24 k A and 72 KA cables, composed of 20 layers of 6 tapes and 30 layers of 12 tapes, respectively. Their engineering current densities without insulation and jacket are 111.9 A/mm^2, 212.8 A/mm^2, and 248.4 A/mm^2. As expected, the current densities are lower than the values in Table I since the former size is much larger.

Table II. Four FReTC conductors designed with 4 mm width, 0.095 mm tape thickness, substrate 0.05 mm REBCO tapes for the former thickness of 4.76 mm.

Cables	a	b	c
The number of strands in a single layer N	4	2	4
The number of filaments in a strand n_s	1	3	3
The number of the total filaments in a single layer cable n_t	4	6	12
Twist pitch (mm)	200	200	200
Surface coverage of filaments (%)	100	100	100
Layer critical current* *Ict* (A)	800	1,200	2.400
Multiple-layer cable			
The number of layers in a cable N_m	5	20	30
The number of the total filaments in a cable n_f	20	120	360
Filament width (mm)	4	4	4
Former thickness (mm)	4.76	4.76	4.76
Former width (mm)	5.31	9.37	22.00
Critical current* *Ic-cable* (A)	4,000	24,000	72,000
Engineering Current density** *Je* (A/mm^2)	111.9	212.8	248.4

* Note: Filament 4 mm width, I_c =200 A at 77 K at cable self-field or at 18 T at 4.2 K.
** Note: Former thickness 4.76 mm and tape thickness 0.095 mm (substrate thickness 0.05 mm). The current density for the former and the REBCO tapes without insulation and jacket.

3.4 Cable fabrication methods

A FReTC will be fabricated quickly and efficiently compared to other flat-tape cabling methods, especially for narrow tapes comparing with other flat tape cablings. In addition, fine-flat-filament tape cables are desired for AC ramp-field and pulse-field applications with low AC losses and low shield currents. A filament can be wound on a round-edge bar former with a given pitch to make multiple filaments and multiple-layer cables. For fine filament flat-cabling, a possible fabrication method with a bundle of the filaments is shown in Fig. 17(a). For example, the 10 filaments bundled on a strand are helically wound on the former. The former can be rotated during winding, or the bundled-tape spools (not shown in Fig. 17) can

be turned around the cable former. Fig. 17(b) illustrates a cabling method of multiple layers of the filament bundles. The figure shows an example of four layers.

A cable former provides mechanical support during a cable fabrication, and also it supports the superconducting conductor against electromagnetic Lorentz force experienced during operation. The filaments, if desired, can be soldered on the former during winding or after the cable winding to support the REBCO tapes mechanically. Common solders are mostly electrically conductive. Therefore, AC losses are increased with the solder, but current sharing can be enhanced.

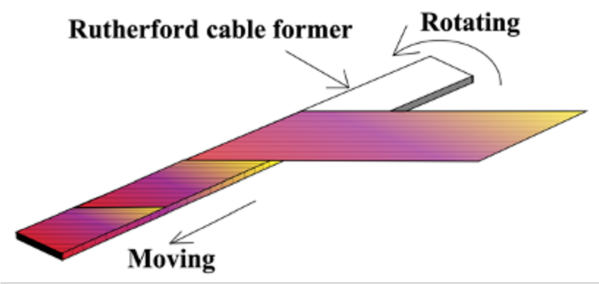

(a)

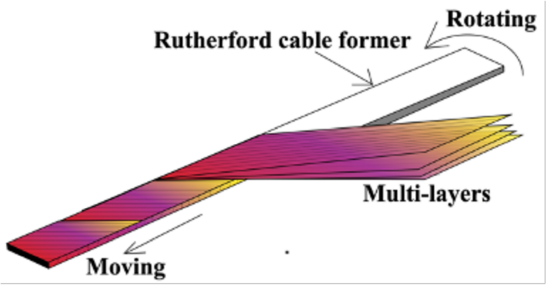

(b)

Fig. 17. (a) A fabrication method of a FReTC. The multiple filaments bundled wound helically on a rotating former. (b) Illustration of a multiple-layer cabling method using filament bundles showing four layers.

3.5 Characteristics of FReTC conductor

When a REBCO tape is wound on a round-edge bar former with keeping the REBCO layer inward (REBCO Inner) during a FReTC cabling, critical-current degradation can be minimized.

Various FReTC conductors are shown in Tables I and II. The cable designs using popular REBCO tapes of 4 mm width and 0.05 mm thick substrate are listed in Table II. A thick cable former of 4.67 mm was used since the former thickness did not degrade the critical current much in the REBCO Inner bending test, as shown in Fig. 4. It was found that the former thickness of about 5 mm is required to wind the REBCO tapes with a substrate of 0.05 mm to minimize cabling degradation. As seen in Table II, the FReTC of an even 4.67 mm thick former will provide more than the engineering current density of 200 A/mm^2 using multiple layers 20 or more. In addition, a thick former will be used to provide an internal cooling channel in the former surrounding with a cable winding.

If a thin substrate REBCO tape is used, a much thinner former will be used for a FReTC conductor. As a result, the engineering current density will be increased. Some examples are shown in Table I, where a substrate thickness is 0.025 mm, and a REBCO tape thickness is 0.035 mm. For the REBCO tape, the former can be 2.5 mm, resulting in a similar bending strain as that for the tested tapes shown in Fig. 4. As seen in Table I, FReTC conductors of 24 kA and 72 kA will be fabricated with the engineering current densities of 590.2 A/mm^2 for 48 layers and 698.9 A/mm^2 for 72 layers, respectively.

It will be desired to make the former thickness thinner to obtain a high current density and good bendability. It will be possible to use an even thinner former (1 mm) for the cabling. A narrower tape width does not theoretically benefit from making the former thinner. However, narrower tapes will make the cabling easier for a thin former. In this case, special attention should be paid to the cable support at the former edges during a cable fabrication. To rigidly support REBCO tapes on a former against electromagnetic and mechanical forces, the tapes can be soldered on the former, and ribs can be helically added on the former, if needed.

A FReTC conductor will be fabricated with a twist-pitch much longer than the former width. As a result, the tape length almost equals the cable length, resulting in good tape usage.

The flat section of a round-edge former can support well REBCO tapes against the transverse force. When a flat tape is wound on a round-edge bar, the length fraction F_r of the flat section to the total tape-length will be given by,

$$F_r = \frac{2\,(W_c - D_e)}{2\,(W_c - D_e) + \pi\, D_e} \tag{15}$$

where W_c is the cable former width, D_e is the cable former thickness (the diameter of the round edge).

The former of the 12.7 mm width, 4.76 mm thick round-edge bar in Fig. 11 has the ratio F_r = 51%. It means that the flat section of the REBCO tape is about half of the total tape length. The flat tape section does not reach the critical current even if the round-edge section does. To minimize a critical current degradation, it is desired to have the ratio F_r larger than 50%. The former thickness D_e should be much smaller than the former width; $W_c >> D_e$. It is important to note that by increasing the former width, the twist-pitch angle becomes large, and the tape usage becomes worse.

3.6 Summary of FReTC conductor

Based on the experimental results of the REBCO tape width-bending, FReTC conductors have been investigated. A REBCO FReTC can provide various advantages, especially for narrow-tape (filament) cabling. The flat cabling has better characteristics against an electromagnetic transverse Lorentz force. Furthermore, the tape length of the cable can be approximately the same as the cable length. Thus, it allows excellent tape usage. REBCO FReTC conductors will be a promising high-current, high-field cabling method with thin substrate REBCO tapes.

In this novel cabling configuration, the tapes (filaments) in the cable are symmetrically wound in parallel. Therefore, the inductance on a filament in the cable can be uniform. Consequently, a uniform current distribution among the cable filaments is obtained.

The cabling method is suitable to develop fine-flat-filament tape cables for AC ramp-field and pulse-field applications with low AC losses and low shield currents. Furthermore, it will

be useful for developing fine-flat-filament tape cables for a high current conductor for AC current applications such as industrial motors and generators, fusion and accelerator machines, and power transmission cables.

The cable can be soldered after winding. The solder is useful for enhancing mechanical support for the tapes, sharing currents, and increasing the stability margin. However, the solder can increase AC losses by increasing coupling currents. Alternately highly resistive solders or non-metallic materials can be selected.

4. Conclusion

It has been found experimentally that the width-bending strain of a YBCO tape does not degrade the critical current as much as is expected from the strain. The effective strain on the critical current seems to be the axial strain, which the width-bending strain generates by the Poisson effect. Since Poisson's ratio is about 0.3, the axial strain effective on the critical current is about 30% of the width-bending strain. Therefore, the width-bending strain does not degrade the critical current much.

Experimentally, it was observed that even 1.5% width-bending strain degraded the critical current by only 15% if the REBCO layer side is bent inward. However, when the REBCO layer is outward, the critical current is degraded by more than 70%. In this work, we demonstrated how these phenomena can be explained considering Poisson's ratio changes and the neutral plane shift of the REBCO tape substrate, corresponding to material yielding due to the severe width-bending.

Following these results, a novel cable configuration of FReTC was proposed. It is possible to fabricate a FReTC of REBCO tapes without significant degradation. REBCO layer should be wound inward on a round-edge flat former. The FReTC conductor can provide various advantages for REBCO tape conductor fabrication. REBCO tapes or bundled narrow-filaments slitting of a REBCO wide tape to narrow filaments can easily be cabled on a former with keeping the REBCO filaments in parallel and wounding along a flat round-edge former.

This cabling technology allows the fabrication of an easy and low-cost high-current cable with HTS fine-flat-wires (filaments). In addition, the cabling method is suitable for developing a high current conductor for AC applications such as industrial motors and generators, fusion and accelerator machines, and power transmission cables.

Furthermore, a FReTC conductor has better characteristics against an electromagnetic transverse Lorentz force, known as an advantage of a Rutherford-type cable. The tape length of a FReTC conductor can be approximately the same as the cable length since it does not require a short twist-pitch.

A FReTC conductor for REBCO tapes is a promising high-current, high-field cabling method. It will also be suitable for a Cable-in-Conduit-Conductor (CICC). Further studies and experimental data are necessary to study in more details the cable design, fabrication method, and a cable support mechanism against large Lorentz forces experienced in a high field.

Acknowledgements

This work was partially supported by the U. S. Department of Energy, Office of Fusion Energy Science under Grants: DE-FC02-93ER54186.

References

[1] W. Goldacker, A. Frank, A. Kudymow, R. Heller, A. Kling, S. Terzieva, and C. Schmidt,

"Improvement of superconducting properties in ROEBEL assembled coated conductors (RACC)," *IEEE Trans. Appl. Supercond*. 19, pp. 3098–3101, 2009.

[2] A. Kario, M. Vojenciak, F. Grilli, A. Kling, B. Ringsdorf, U. Walschburger, S. I. Schlachter, and W Goldacker, "Investigation of a Rutherford cable using coated conductor Roebel cables as strands," *Supercond. Sci. Technol*., 26, 085019 (6pp), 2013.

[3] D.C. van der Laan, P.D. Noyes, G.E. Miller, H.W. Weijers, and G.P. Willering, "Characterization of a high-temperature superconducting conductor on round core cables in magnetic fields up to 20 T," *Supercond. Sci. Technol*., 26, 045005, 2013.

[4] M. Takayasu, L. Chiesa, L. Bromberg, and J.V. Minervini, "HTS twisted stacked-tape cable conductor," *Supercond. Sci. Technol*., 25, 014011, 2012.

[5] M. Takayasu, J.V. Minervini, L. Bromberg, M.K. Rudziak, and T. Wong, "Investigation of twisted stacked-tape cable conductor," *Adv. Cryo. Eng*. 58 Plenum, N.Y., pp. 273-280, 2012.

[6] G. Celentano, G. De Marzi, F. Fabbri, L. Muzzi, G. Tomassetti, A. Anemona, S. Chiarelli, M. Seri, A. Bragagni, and A. della Corte, "Design of an Industrially feasible twisted-stacked HTS cable-inconduit conductor for fusion application," *IEEE Trans. Appl. Superconduct*, 24 4601805, 2014.

[7] D. Uglietti, R. Wesche, and P. Bruzzone, "Design and strand tests of a fusion cable composed of coated conductor tapes," *IEEE Trans. Appl. Superconduct,* 24 4800704, 2014.

[8] N. Yanagi, et al., "Design and development of high-temperature superconducting magnet system with joint-winding for the helicalfusion reactor," *Nucl. Fusion*, 55, 053021 (7pp), 2015.

[9] M. J. Wolf, W. H. Fietz, C. M. Bayer, S. I. Schlachter, R. Heller, and K. P. Weiss, "HTS CroCo: A Stacked HTS Conductor Optimized for High Currents and Long-Length Production," *IEEE Trans. Appl. Superconduct*, 26, 6400106, 2016.

[10] M. Takayasu, F.J. Mangiarotti, L. Chiesa, L. Bromberg, and J.V. Minervini, "Conductor characterization of YBCO twisted stacked-tape cables, "*IEEE Trans. Appl. Superconduct*, 23, 4800104, 2013.

[11] Z. S. Hartwig, et al. "VIPER: an industrially scalable high-current high-temperature superconductor cable," *Supercond. Sci. Technol*., 33, 11LT01, 2020.

[12] W. Pi, S. Ma, Q. Kang, Z. Liu, Y. Meng, and Y. Wang, "Study on mechanical properties of quaasi-isotropic superconducting strand stacked by 2-mm-wide REBCO and copper tapes," *IEEE Trans. Appl. Superconduct*, 30, 6600105, 2020.

[13] D. Uglietti, "A review of commercial high temperature superconducting materials for large magnets: from wires and tapes to cables and conductors," *Supercond. Sci. Technol*. 32 053001, 2019.

[14] M.N. Wilson, "*Superconducting Magnets*," Oxford University Press, Clarendon Press Publication, 1987.

[15] N. Andreev, E. Barzi, E. Borissov, L. Elementi, V. S. Kashikhin, V. Lombardo, A. Rusy, D. Turrioni, R. Yamada, and A. V. Zlobin, "Development of Rutherford-Type Cables for High Field Accelerator Magnets at Fermilab," *IEEE Trans. Appl. Supercond*. 17, pp. 1027–1030, 2007.

[16] T. Hasegawa, J. Nishioka, N. Ohtani, Y. Hikichi, R. Scanlan, R. Gupta, N. Hirano, and S. Nagata, "12 kA HTS Rutherford cable," *IEEE Transactions on Applied Superconductivity*, vol. 14, No. 2, pp. 1066-1069, 2004.

[17] S.I. Schlachter, W. Goldacker, F. Grilli, R. Heller, and A. Kudymow, "Coated conductor Rutherford Cables (CCRC) for high-current applications: Concept and properties," *IEEE Trans. Appl. Supercond.* 21, pp. 3021–3024, 2011.
[18] D. C. van der Laan and J.W. Ekin, "Dependence of the critical current of YBa2Cu3O7−δ coated conductors on in-plane bending," *Supercond. Sci. Technol.*, 21, 115002, 2008.
[19] J.M. Gere and S.P. Timoshenko, *Mechanics of Materials*, 2nd ed., PWS Publishers, Boston, Massachusetts, 1984.
[20] For example, Poisson's ratio, https://en.wikipedia.org/wiki/Poisson%27s_ratio, Wikipedia.
[21] M. Takayasu, L. Chiesa, D. L. Harris, A. Allegritti, and J. V. Minervini, "Pure bending strains of Nb_3Sn wires," *Supercond. Sci. Technol*., 24, 045012 (16p), 2011.
[22] J. W. Ekin, "Strain scaling law and the prediction of uniaxial and bending strain effects in multifilamentary superconductors," Filamentary A15 Superconductors: Proc. Tropical Conf. on A15 Superconductors ed M Suenaga and A Clark (New York: Plenum) pp 187–203, 1980.
[23] K. Kaiho, T. S. Luhman, M. Suenaga and W. B. Sampson, "Effects of bending on the superconducting critical current density of monofilamentary Nb3Sn wires," *Appl. Phys. Lett*. 36 223–5, 1980.
[24] Y. Kubo and T. Ozawa, "Derivation of Ic degradation rate for reacted Nb3Sn wires under applied bending and tensile strains," *Cryog. Eng. J. Cryog. Soc*. Japan 37 68–76, 2002.
[25] D. C. van der Laan, X. F. Lu and L. F. Goodrich, "Compact GdBa2Cu3O7–δ coated conductor cables for electric power transmission and magnet applications," *Supercond. Sci. Technol.*, 24, 042001, 2011.
[26] C.C. Clickner, J.W. Ekin, N. Cheggour, C.L.H. Thieme, Y. Qiao, Y.-Y. Xie, A. Goyal, "Mechanical properties of pure Ni and Ni-alloy substrate materials for Y–Ba–Cu–O coated superconductors," *Cryogenics*, 46, 432–438, 2006.
[27] K. Han, J. Chen, R. E. Goddard, W. D. Markiewicz, V. J. Toplosky, and R. P. Walsh, "Mechanical Properties of Non-Superconducting Components in YBCO and Nb_3Sn Composites," *IEEE Trans. Appl. Superconduct*, 21, 3119-3122, 2011.
[28] T. Luhman and D. O. Welch, "Studies of strain-dependent properties of A15 filamentary conductors at Bbrookhaven National Laboratory," Filamentary A15 Superconductors: Proc. Tropical Conf. on A15 Superconductors ed M Suenaga and A Clark (New York: Plenum) pp 171–186, 1980.
[29] T. Okada, H. Misaizu, and S. Awaji, "In-Plane Domain Control of REBCO Coated Conductors by Annealing Under Bending Strain," *IEEE Trans. Appl. Superconduct*, 31, 6601006, 2021.
[30] S. Kar et al., "Progress in scale-up of REBCO STAR™ wire for canted cosine theta coils and future strategies with enhanced flexibility," *Supercond. Sci. Technol*., 33, 094001 (16pp), 2020.
[31] V. Solovyov and P. Farrell, "Exfoliated YBCO filaments for second-generation superconducting cable," *Supercond. Sci. Technol*., vol. 30, 014006, 2017.